# Electronic structure changes across the valence transition in $EuNi_2(Si_{0.2}Ge_{0.8})_2$

P. A. Rayjada,[1,2] A. Chainani,[2,3] K. Kanai,[3,4] T. Haruna,[1] T. Yokoya,[1] S. Shin,[1,3] H. Wada,[5] and M. Shiga[5]
[1]*Institute for Solid State Physics, University of Tokyo, Kashiwa, Chiba 277-8581, Japan*
[2]*Institute for Plasma Research, Bhat, Gandhinagar, 382 428, India*
[3]*RIKEN/SPring-8, 1-1-1 Kouto, Mikazuki-cho, Sayo-gun, Hyogo 679-5148, Japan*
[4]*Department of Chemistry, Nagoya University, Nagoya 464-8602, Japan*
[5]*Department of Materials Science and Engineering, University of Kyoto, Kyoto 606-8501, Japan*
(Received 11 December 2003; revised manuscript received 20 August 2004; published 1 December 2004)

We study the electronic structure of $EuNi_2(Si_{0.2}Ge_{0.8})_2$, which exhibits a temperature dependent mixed valence transition, using $4d$-$4f$ resonant photoemission spectroscopy (RESPES), x-ray absorption spectroscopy (XAS) and temperature-dependent ultraviolet photoemission spectroscopy (UPS). The RESPES studies identify the divalent and trivalent Eu $4f$ character density of states (DOS) which participate in the valence transition. Using the photoionization cross section variation as a function of photon energy, we discuss the Eu, Ni, and Ge-Si partial DOS in the valence band. The bulk divalent Eu $4f$ character states are centered at a binding energy of about 0.75 eV, significantly away from the Fermi level. While the surface divalent feature is negligibly affected, the spectra obtained using He II$\alpha$ UPS exhibit temperature dependent bulk Eu $4f$ character states. The bulk divalent spectral weight is transferred to the high energy trivalent states, across the valence transition temperature, $T_v \sim 80$ K. The He I$\alpha$ UPS also exhibit spectral intensity changes across $T_v$. The non-$f$ character conduction band states at and near the Fermi level exhibit spectral weight changes up to 350 meV with a small energy ($\sim$25 meV) temperature dependent pseudogaplike feature. The results suggest an increase in effective hybridization strength between the conduction and $4f$ electrons in the low temperature nearly trivalent phase. While the $4f$ character changes across $T_v$ are qualitatively consistent with change in valence configurations, the temperature dependent spectral changes in the non-$f$ character DOS indicate direct participation in the valence transition in $EuNi_2(Si_{0.2}Ge_{0.8})_2$.

DOI: 10.1103/PhysRevB.70.235105 PACS number(s): 71.28.+d, 75.30.Mb, 79.60.Bm

## I. INTRODUCTION

Many Europium based intermetallic compounds exhibit a temperature dependent mixed valence transition.[1–11] These compounds exhibit a relatively large change in valence as a function of temperature, stoichiometry (chemical pressure), pressure and magnetic field from a nearly divalent to a nearly trivalent state. Early studies interpreted the experimental results in terms of the interconfiguration fluctuation (ICF) model on the basis of the energy-proximity of the magnetic ($J=7/2$, eightfold degenerate) Eu $4f^7$ (divalent) and nonmagnetic ($J=0$, singlet) $4f^6$ (trivalent) states with quantum mechanical mixing of the two states.[1,4,12] This model required a phenomenological correction known as cooperative ICF in the form of a nonlinear temperature dependent energy separation ($E_{ex(T)}$) of the aforesaid two valence states in order to describe the rapid (first-orderlike) valence transition observed in $EuPd_2Si_2$ (Ref. 5) and $EuNi_2(Si_{0.2}Ge_{0.8})_2$ (Refs. 7 and 8). It was suggested that this dependence can come from electronic or elastic energy change of the system.[3,5] Electronic Raman scattering of $EuPd_2Si_2$ confirmed that it is the two-state mixing, which is changing with temperature.[6]

In an alternative approach to the mixed valence transition, it was suggested that conduction-electron screening of the local charge at the trivalent site and hence, the density of states at and near the Fermi-level (DOS($E_F$)), can be a key factor to determine the stability of the $4f$ configuration in Eu compounds.[13] This would imply a change in the DOS($E_F$) as a function of temperature could play an important role in the transition. As discussed in Ref. 13, this approach parallels the work by Haldane[14] for Ce compounds using the Anderson impurity-model with a Falicov-Kimball term to reproduce the screening effect. The Kondo volume collapse (KVC) model for the Ce $\alpha$-$\beta$ isostructural first-order valence transition also predicts that higher DOS($E_F$) would effectively increase $f$-electron to conduction-band ($f$-$c$) hybridization strength in the lower volume (nonmagnetic), low temperature phase in order to gain Kondo energy against elastic energy loss.[15] The single impurity Anderson model (SIAM) has been applied extensively to understand properties of Ce and Yb based rare-earth compounds, with electron spectroscopy studies playing a significant role.[16] More recently, solutions of the periodic Anderson model (PAM),[17–19] the Kondo lattice model[20] and the Falicov-Kimball (FK) model[21] have provided important insights for rare-earth systems. In particular, these studies address issues relating to dispersive $f$-bands, exhaustion physics, and the Kondo and coherence scales in materials spanning from Kondo insulators to mixed valent systems. First principles calculations[22] have also addressed the issue of mixed valence in Sm, Eu, Tm, and Yb compounds and indicate that the mixed valence transition occurs between two states which are close in energy (e.g., in SmS, the mixed valence transition as a function of pressure occurs between states with an energy difference of $\sim$15 meV, which is of the order of room temperature). Most importantly, both the states actually consist of fully occupied integral number of localized $f$-electrons which determine its

 

magnetism and nonintegral delocalized $f$-electrons which are strongly hybridized with the non-$f$ character $s$-$d$ bands. It was also shown from a PAM study of SmS in the local density approximation that the semiconducting black phase of SmS exhibits mixed valency.[23] This was confirmed by experiments and temperature dependent PES studies suggested that the divalent to trivalent ratio changes as a function of temperature, along with changes in the DOS ($E_F$).[24] Since $EuNi_2(Si_{0.2}Ge_{0.8})_2$ exhibits a mixed-valence transition similar to SmS, we felt it important to study it using electron spectroscopy. Interestingly, two independent and different theoretical approaches based on PAM (Refs. 17–19 and 25) and FK model[21] require the parameter $E_{4f}$ [energy position of $4f$ level with respect to Fermi-level ($E_F$)] to change with temperature or applied pressure in order to reproduce a large and rapid valence change. The large valence change puts Eu compounds in the mixed-valent regime of the Anderson model.[25] Also, the FK approach predicts a pseudogap at $E_F$ in the high-temperature nearly-divalent phase of systems showing a mixed valence transition such as $EuNi_2(Si_{1-x}Ge_x)_2$ (Ref. 21).

$EuNi_2(Si_{1-x}Ge_x)_2$ has the tetragonal $ThCr_2Si_2$ crystal structure and it is normally considered that Eu is divalent for $x=1$ and trivalent for $x=0$ (Ref. 26). It has been shown by temperature-dependent magnetic susceptibility, $L_{III}$ edge absorption, resistivity and lattice parameter measurements that the compound in the range $0.5<x<0.82$, undergoes a temperature-driven valence transition from a valence of $\sim 2.2-2.3$ to $\sim 2.7-2.8$, accompanied by quenching of local magnetic moment and unit-cell volume change as high as 5 Å$^3$ (Refs. 8 and 9). For $x>0.82$, the system undergoes antiferromagnetic (AF) ordering at approximately 40 K at ambient pressure, whereas a stable trivalent phase is found for $x<0.5$. The valence transition temperature ($T_v$) sensitively depends on $x$. In particular, critical concentrations in the vicinity of AF phase boundary ($x\sim 0.8$) show the largest changes in properties across the valence transition.[9] The electrical resistivity ($\rho$) data of $EuNi_2(Si_{0.2}Ge_{0.8})_2$ shows a sharply reduced $\rho$ in the low temperature phase across the mixed valence transition, but is metallic both above and below the transition with an anomaly (upturn) at the valence transition temperature, $T_v\sim 80$ K. From a combined pressure and doping dependent study, it was concluded that the temperature dependence of $\rho$ is best explained by impurity scattering due to randomness in a virtual alloy, within the cooperative ICF model.[10] The thermoelectric power also shows a gradual anomaly at the valence transition temperature,[27] but no clear jump suggesting that the carriers do not change discontinuously at $T_v$. The AF transition temperature ($T_N$) remains nearly constant for $0.82>x>1$ suggesting that Kondo coupling constant may not be as important as in elemental Ce.[15] However, even for $x=0.85$ and $x=1$ compounds, which are known to be AF below 40 K at ambient pressure, a first-order-like valence transition is revealed under high pressure.[10]

In this work, we report ultraviolet photoemission spectroscopy (UPS) measurements on $EuNi_2(Si_{0.2}Ge_{0.8})_2$ in combination with resonant photoemission spectroscopy (RESPES) and x-ray absorption spectroscopy (XAS) measurements. Photoemission spectroscopy on this compound is challenging due to the high reactivity of $f$-electron materials demanding extreme care in sample surface preparation and measurement in order to avoid spurious surface effects. However, UPS studies on another mixed valent compound, $YbInCu_4$, have shown that while the temperature dependent valence transition is not as sharp as in bulk sensitive measurements, it is possible to measure the intrinsic valence change in such materials.[28] While a recent study of $4d$-$4f$ RESPES on scraped surfaces[11] showed no evidence of the mixed valency, the present study on fractured surfaces provides clear evidence of mixed valency. Photoionization cross-section variation as a function of photon energy[29] is used to discuss the Eu, Ni, and Ge-Si partial DOS in the valence band. Using $4d$-$4f$ resonance, we identify bulk and surface divalent Eu $4f$ features and the bulk trivalent Eu $4f$ features in the valence band spectra. Temperature dependent He II$\alpha$ UPS shows a valence change in the form of spectral weight transfer from Eu divalent to trivalent features across $T_v$. The He I$\alpha$ UPS shows that the non-$f$ character DOS also exhibit spectral intensity changes across $T_v$. The near $E_F$ spectra shows increase in non-$f$ character DOS within $\sim 350$ meV of $E_F$ as temperature is reduced across $T_v$, indicating increasing strength of $f$-$c$ hybridization. A symmetrization analysis to remove temperature effects reveals a pseudogaplike feature located at $E_F$. The temperature dependent spectral changes in the $f$ and non-$f$ character states indicate coupled changes across the valence transition in $EuNi_2(Si_{0.2}Ge_{0.8})_2$.

## II. EXPERIMENT

Polycrystalline samples of $EuNi_2(Si_{0.2}Ge_{0.8})_2$ were prepared and characterized as described in Ref. 8. Since as-cast samples show a sharper valence transition as a function of temperature compared to annealed samples, we used as-cast samples with a $T_v\sim 80$ K for the measurements. XAS and RESPES across the $4d$-$4f$ threshold were performed at beamline 19-B of Photon Factory, Tsukuba, Japan. XAS and RESPES spectra were measured within 80 min of cleaving and the base pressure was $2\times 10^{-10}$ Torr. XAS was carried out in the total-fluorescence-yield mode on freshly fractured surfaces at room temperature, at a resolution of 0.8 eV. The total energy resolution for RESPES spectra was 0.2 eV as determined from the $E_F$ of a gold film evaporated onto the sample substrate. Temperature-dependent angle-integrated UPS was carried out using monochromatized He I$\alpha$ and He II$\alpha$ radiation from GAMMADATA discharge lamp and Scienta SES 2002 analyzer at a base vacuum of $9\times 10^{-11}$ Torr at ISSP, Japan. The energy resolutions for He II$\alpha$ valence band data, He I$\alpha$ valence band and near $E_F$ data were set to $\sim 300$, $\sim 30$, and 15 meV, respectively. $E_F$ was referred to that of gold film evaporated onto the sample substrate and measured with an accuracy of $\sim 0.5$ meV. Temperature of the sample was measured using a calibrated silicon diode sensor and was controlled using a local heater and a flowing liquid helium cryostat equipped with thermal shielding. To check reproducibility of temperature dependent data, we fractured the sample at room temperature and then

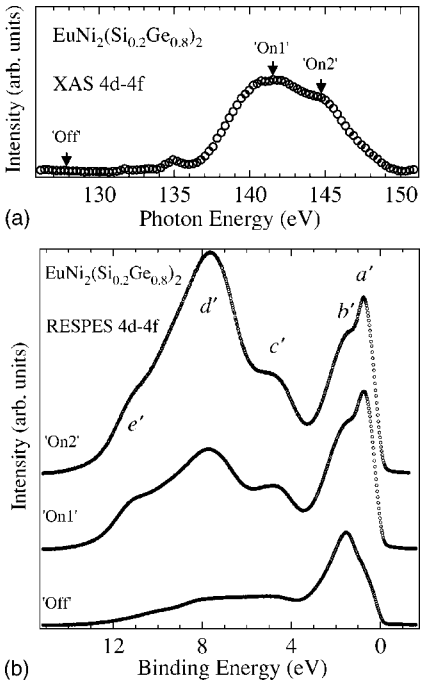


FIG. 1. (a) X-ray absorption spectrum of $EuNi_2(Si_{0.2}Ge_{0.8})_2$ at room-temperature across the $4d$-$4f$ threshold measured in total-fluorescence yield mode. (b) Resonant photoemission spectra at room-temperature across the $4d$ threshold at photon energies labeled 'Off, 'On1,' and 'On2' in the XAS spectrum in (a).

measured in a temperature cycle from 300 to 10 K and back to 300 K. To obtain rapid cool-down required due to limited surface lifetime, we first cooled down the sample holder, maintaining the sample at room temperature with the local heater and after achieving cooling of the sample holder, the sample was fractured and rapidly cooled. The presented results were also reproducibly obtained on several fractured samples cut from the same ingot. The UPS spectra were recorded within 2 h of fracture and no changes in the spectra were observed due to surface degradation/contamination within this period.

### III. RESULTS AND DISCUSSIONS

Figure 1(a) shows XAS measured in the total-fluorescence-yield mode across the Eu $4d$ threshold of $EuNi_2(Si_{0.2}Ge_{0.8})_2$ at room temperature. An integral background has been subtracted from the raw spectrum. The spectrum shows two prepeaks, a weak one at ~132 and a clear feature at 135 eV, followed by the main peak at 141.5 eV and shoulder at 145 eV. The main peak is assigned to $4d^9 4f^8$ ($Eu^{2+}$ initial state) and the shoulder is due to $4d^9 4f^7$ ($Eu^{3+}$ initial state) states. The main peak and shoulder spectral shape is similar to XAS of $EuNi_2(Si_{0.25}Ge_{0.75})_2$ across the $3d$ and the $2p$ thresholds, which also show a main peak and a shoulder and have been assigned to the $4f^7(Eu^{2+})$ and $4f^6(Eu^{3+})$ initial states. Figure 1(b) shows the raw 'Off' and 'On'-resonance photoemission spectra obtained with high-signal to noise ratio at photon energies of 127, 141.5, and 145 eV, labeled as 'Off,' 'On1' and 'On2' in Fig. 1(a). The RESPES spectra are normalized to the incident photon flux. The off-resonance spectrum is similar to the valence band spectrum observed with a high photon energy ($h\nu = \sim 1100$ eV, Ref. 11). Atomic photoionization cross sections (PICS) indicate that, at about the off-resonance energy used,[29] the Ni $3d$ states are comparable to Eu $4f$ states and which are typically an order of magnitude higher than the Ge-Si $sp$ states. The spectrum shows a feature at 1.6 eV with a shoulder at 0.75 eV feature. The surface shifted feature in Eu compounds is well known.[30–34] The 0.75 eV feature corresponds to 'bulk' $Eu^{2+}$ $4f$ states while the 'surface' $Eu^{2+}$ $4f$ feature occurs at 1.6 eV, with Ni $3d$ states spread between 1–3 eV binding energy.[35,36] Very weak features are also found in the range of 4–12 eV and we discuss its origin in the following. On increasing the photon energy to 'On1,' the bulk $Eu^{2+}$ shoulder undergoes a sharp resonant enhancement while the surface feature is not significantly enhanced, resulting in an inversion of intensities with the bulk feature centered at 0.75 eV exhibiting higher intensity. The higher energy features are also enhanced between 4–12 eV, with broad features at about 5, 8, and 11 eV. The feature at 5 eV is attributed to the 'spin-flip' satellites of $Eu^{2+}$ while the higher energy features are attributed to $Eu^{3+}$ features.[11,34] This assignment is based on atomic fractional parentage calculations starting with the initial states of $4f^7$ ($^8S_{7/2}$) and $4f^6$ ($^7F_0$) corresponding to $Eu^{2+}$ and $Eu^{3+}$, respectively. The spin-flip satellite was shown to be resonantly enhanced at and above photon energies corresponding to the prepeak occuring just below the main peak in Gd and SmS, which possess the same $f$-electron configurations as in the present case.[34] Further increase in excitation energy to 'On2,' corresponding to the shoulder in the XAS spectrum, clearly enhances the $Eu^{3+}$ features, without any apparent further enhancement of $Eu^{2+}$ features. The spectrum thus confirms the mixed valency, with features $a'$ and $b'$ for the bulk and surface divalent, $c'$ for the spin-flip states and $d'$ and $e'$ for the trivalent features as labeled in Fig. 1(b).

Due to the significant changes in atomic PICS with changing photon energy[29] between He I$\alpha$ ($h\nu = 21.218$ eV) and He II$\alpha$ ($h\nu = 40.80$ eV) photons, we first compare the UPS spectra of $EuNi_2(Si_{0.2}Ge_{0.8})_2$ with the RESPES data. Figure 2 shows the He I$\alpha$ and He II$\alpha$ UPS data obtained at 150 K along with the He I$\alpha$ spectrum of 10 K. In the high temperature phase above $T_v \sim 80$ K, the He I$\alpha$ and He II$\alpha$ spectra show very different spectral features. The He II$\alpha$ spectrum is similar to the 'Off' resonance spectrum of Fig. 1(b), with clearly separated bulk (0.75 eV) and surface (1.6 eV) $Eu^{2+}$ features which overlap the Ni $3d$ states between 1 to 3 eV binding energy The He I$\alpha$ ($h\nu = 21.218$ eV) spectrum is substantially different compared to the He II$\alpha$ spectrum at the same temperature, with three prominent features at 1.3, 2.1, and 2.6 eV binding energy. The relative change in atomic PICS suggest a strong reduction of the Eu $4f$ states at $h\nu = 21.218$ eV (Ref. 29). Also, the Ge and Si $sp$ states are approximately an order of magnitude smaller than Ni $3d$ states, and usually manifest as a broad featureless background.[30–33] In the absence of band structure calculations for $EuNi_2(Si_{0.2}Ge_{0.8})_2$ we compare the

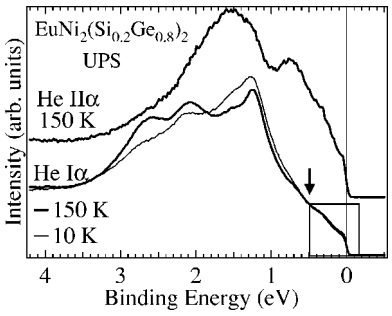


FIG. 2. He I$\alpha$ and He II$\alpha$ comparison of the valence band of $EuNi_2(Si_{0.2}Ge_{0.8})_2$ measured in the high temperature phase ($T$=150 K). The He II$\alpha$ spectrum is dominated by Eu $4f$ states while the He I$\alpha$ spectrum is dominated by Ni $3d$ derived states. Also shown is the low temperature He I$\alpha$ valence band spectrum ($T$=10 K, thin curve).

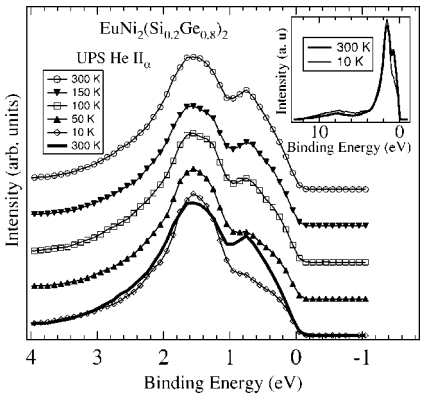


FIG. 3. Temperature-dependent valence-band spectra of $EuNi_2(Si_{0.2}Ge_{0.8})_2$ measured with He II$\alpha$ photons. Inset shows the 10 K and 300 K data over the entire valence band, to show the normalization procedure of the area under the curve for the measured energy range.

data with the calculated DOS (Refs. 35 and 36) for isostructural $LaNi_2Ge_2$ and $CeNi_2Ge_2$. The available band structure calculations suggest that the features observed between 1–3 eV binding energy in $EuNi_2(Si_{0.2}Ge_{0.8})_2$ can be attributed to the Ni $3d$ DOS in the presence of a tetrahedral crystal-field splitting with $e_g$ features ($d_{x2-y2}$ and $d_{z2}$ at 2.1 and 2.6 eV) and the $t_{2g}$ ($d_{xy}$, $d_{yz}$, and $d_{zx}$) derived states centered at 1.3 eV. The spectrum also shows a very low intensity feature within 0.5 eV of $E_F$ with a clear $E_F$-crossing. In a recent angle-resolved PES study[36] of isostructural $CeNi_2Ge_2$ (which is a heavy-fermion compound but does not exhibit a mixed valence transiton), it was shown that the Ni $3d_{xy}$ and Ce $5d_{x2-y2}$ states lie within 0.5 eV of $E_F$. In the present case, the strong reduction in intensity between the feature at 1.3 eV and within 0.5 eV of $E_F$ suggests weak Ni $3d$ character DOS within 0.5 eV of $E_F$, although band structure calculations[35,36] for $CeNi_2Ge_2$ indicate a sharp feature of Ni $3d_{xy}$ character to lie at about 0.4 eV. However, as concluded for $CeNi_2Ge_2$, the He I$\alpha$ data suggests non-$f$ character DOS to lie within 0.5 eV of $E_F$, possibly with significant Eu $5d$ as the well as the Ge-Si $sp$ character.

The temperature dependence between 150 K and 10 K across $T_v \sim 80$ K also shows changes of the VB features using He I$\alpha$ photons ($h\nu$=21.218 eV). The spectra are normalized by scan time and effectively results to normalized area under the curve upto the background intensity at 4 eV. The temperature dependence indicates spectral intensity changes-between the $e_g$ and the $t_{2g}$ derived states. The result suggests that the Ni $3d$ states also directly participate in the transition across $T_v \sim 80$ K. The volume contraction across $T_v \sim 80$ K may be expected to increase the Ni $3d$ bandwidth. Although a clear increase in bandwidth is not easy to identify from the data, the leading edge of the 1.3 eV feature is shifted to slightly lower binding energy. The arrow at 0.5 eV marks the binding energy position with no change in spectral intensity as a function of temperature. We later discuss temperature dependent spectral changes at and near $E_F$ marked by the box up to 0.5 eV, obtained with higher resolution He I$\alpha$ measurements.

As the He II$\alpha$ valence band spectrum in the high temperature phase indicated features due to $4f$ character states, we attempted to see the mixed valence transition as a function of temperature. Figure 3 shows the valence band spectra between 0–4 eV obtained using He II$\alpha$ ($h\nu$=40.814 eV) photons between 300 and 10 K. The spectra are normalized to area under curve over the entire valence band (0–13 eV binding energy) after subtracting an integral background from the raw spectra, as shown in the inset for the 10 K and 300 K spectra. The data at various temperatures are plotted with a constant vertical shift for clarity in the main panel, and in addition the 300 K spectrum is also superimposed on the 10 K spectrum to emphasize the changes. The bulk $Eu^{2+}$ feature at 0.75 eV, which is well separated from the more intense surface $Eu^{2+}$ feature at 1.6 eV, shows temperature dependence, with no change in its binding energy. As temperature is reduced from room temperature, the bulk $Eu^{2+}$ feature seems to show a small reduction in intensity, but across $T_v \sim 80$ K, it clearly loses weight. Since the spectra are normalized for area under the curve over the entire valence band, in order to see the spectral weight transfer, we plot the region between 4 and 12 eV binding energy on an expanded scale in Fig. 4(a) without a constant vertical shift. While the spectral changes are small, the data falls into two sets, clearly separated between the 50 and 100 K spectra.

In order to clearly see the temperature dependent change between 100 K and 50 K, we plot a difference spectrum in Fig. 4(b). The spectral weight is seen to be transferred from the bulk $Eu^{2+}$ features to spin-flip and $Eu^{3+}$ features. The spin-flip state ($4f^{5\uparrow,1\downarrow}$) is an intermediate state lying between the ($4f^{6\uparrow}$) and ($4f^{5\uparrow}$) final states of $Eu^{2+}$ and $Eu^{3+}$ initial states, respectively.[34] Thus, in the temperature dependent transition transferring spectral weight from $Eu^{2+}$ to $Eu^{3+}$, the experimental result indicates that even the spin-flip intermediate state gets populated across the transition. The zero intensity in the difference spectrum at 1.6 eV shows that the surface $Eu^{2+}$ feature does not participate in the transition. The low intensity feature between $\approx$2–3 eV reflects the temperature dependent changes also seen in the He I$\alpha$ data. Note also that the changes in the He II$\alpha$ spectra indicate that the bulk divalent $f$-character states lie just below $E_F$ and do

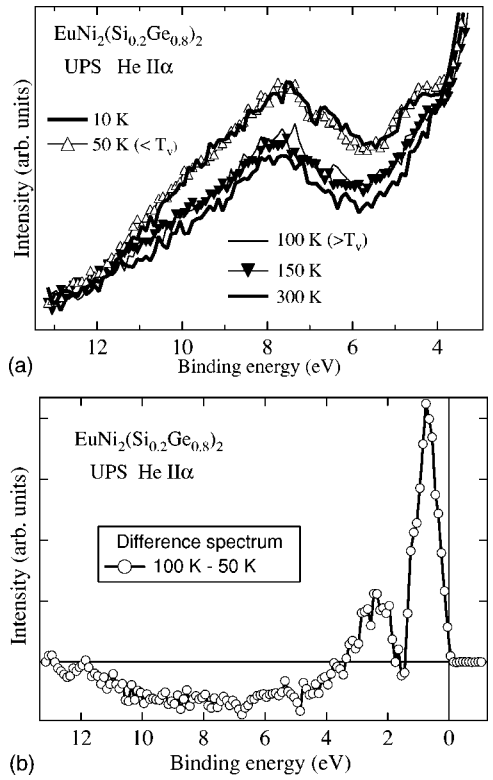


FIG. 4. (a) Valence band curves superimposed on one-another showing the temperature-dependence of trivalent features across the valence transition at 80 K. (b) Shows a difference spectrum between 100 and 50 K, indicating spectral weight transfer between Eu bulk-divalent (0.75 eV) and the spin-flip and trivalent (4–12 eV) features.

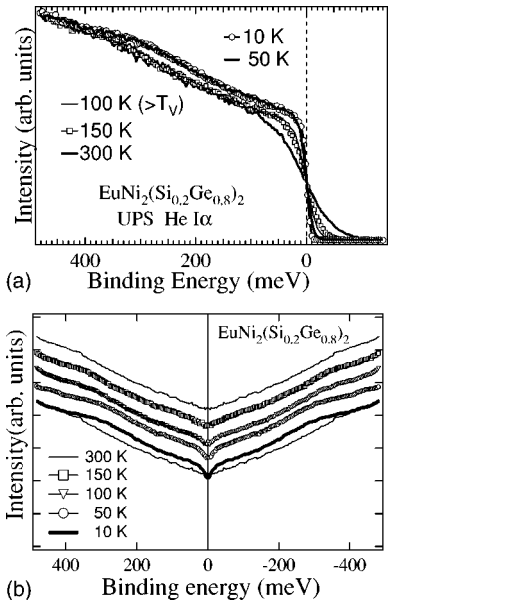


FIG. 5. (a) Temperature-dependent (10–300 K) He I$\alpha$ spectra of $EuNi_2(Si_{0.2}Ge_{0.8})_2$ near $E_F$ showing increase in DOS within ~350 meV of $E_F$ on reducing temperature. (b) Symmetrized spectra (10–300 K) shows a pseudogaplike feature at $E_F$. The 300 K spectrum is also overlaid on the 10 K spectrum to show negligible change in intensity at $E_F$.

not cross it, corresponding to a gap in the $f$-character DOS. The results indicate that even low energy UPS can be used to study the mixed valence transition in $f$-electron systems, although UPS is very surface sensitive. However, due to the presence of the surface divalent state feature which does not show temperature dependence, a comparison with the valency change obtained from other bulk physical property measurements is not possible.

Next we discuss the temperature dependence of high-resolution data near $E_F$ measured with He I$\alpha$ photons and consisting of non-$f$ (Eu 5$d$ as well as Ge-Si $sp$ character) conduction band DOS as shown in Fig. 5(a). The spectra are normalized to the intensity at 0.5 eV, the point where no changes in spectral intensity were observed as a function of temperature between 10 and 150 K, as shown in Fig 2. The spectra show an increase in DOS within ~350 meV of $E_F$ as temperature is reduced across $T_v$. The increased DOS is suggestive of increasing 4$f$-conduction electron hybridization strength in the low temperature phase. In order to see the changes in the DOS ($E_F$) without Fermi-Dirac broadening, we symmetrize the spectra and plot with a constant vertical shift as shown in Fig. 5(b). This numerical procedure removes temperature effects which are symmetric about the zero of the binding energy scale and gives the change in the density of states within $\sim 5k_BT$ of $E_F$ without temperature effects.[37] The analysis shows that the spectral weight changes as a function of temperature lead to a pseudogaplike structure at $E_F$ of ~25 meV, accompanying the spectral changes at higher energies. But a plot of the 300 K spectrum superimposed on the 10 K symmetrized spectrum i.e., without a constant vertical shift, indicates negligible change in intensity at $E_F$. While this seems contradictory to the reduced resistivity in the low temperature phase, the temperature dependent resistivity data has been analyzed in terms of a change in the impurity scattering due to randomness in a virtual alloy, within the cooperative ICF model. Hence it is not necessary for the DOS ($E_F$) to change as a function of temperature. Note also that the pseudogap in the conduction band DOS expected in the FK model in the high temperature phase is supposed to be weaker or absent in the low temperature phase. In the present data, the pseudogaplike feature is more pronounced in the low temperature phase [Fig. 5(b)]. The changes in the DOS at and near $E_F$ suggest importance of two energy scales, of ~25 meV and ~350 meV. Recent theory has shown that for the case of Kondo lattice materials, there exist two energy scales associated with spectral changes near the Fermi level in low carrier systems. A low energy scale related to the coherence temperature and a higher energy scale indicating the Kondo temperature.[19,20] The spectral changes observed in the present case are also similar to that observed in the mixed valent system SmS,[24] and in analogy, we suggest that the observed behavior is similar to that calculated for low carrier Kondo lattice systems.[19,20]

## IV. CONCLUSIONS

In conclusion, the RESPES data neatly identifies all Eu 4$f$ features: surface and bulk divalent, trivalent, and the spin-

flip features, in the valence band spectra of $EuNi_2(Si_{0.2}Ge_{0.8})_2$. Temperature dependent He II$\alpha$ UPS valence band spectra show the valence transition occurring between 100 and 50 K. However, due to the surface sensitivity of the technique and the presence of the surface divalent state feature which does not show temperature dependence, a comparison with the valency change obtained from other bulk physical property measurements is not possible. He I$\alpha$ UPS valence-band spectra show temperature dependent changes consistent with the volume contraction. The Ni 3*d*-derived features exhibit crystal field split $e_g$ and $t_{2g}$ states. High-resolution, near $E_F$ temperature-dependent He I$\alpha$ UPS suggests increasing *c*-*f* hybridization strength as temperature is lowered below $T_v$. While the 4*f* character changes across $T_v$ are qualitatively consistent with change in valence configurations, the temperature dependent spectral changes in the non-*f* character states indicate direct participation in the valence transition in $EuNi_2(Si_{0.2}Ge_{0.8})_2$.

## ACKNOWLEDGMENT

P.A.R. thanks the Monbukagakusho (Japan) for a visiting fellowship.

[1] B. C. Sales and D. K. Wohlleben, Phys. Rev. Lett. **35**, 1240 (1975).
[2] E. V. Sampathkumaran, L. C. Gupta, R. Vijayaraghavan, K. V. Gopalakrishnan, R. G. Pillay, and H. G. Devare, J. Phys. C **14**, L237 (1981).
[3] C. U. Segre, M. Croft, J. A. Hodges, V. Murgai, L. C. Gupta, and R. D. Parks, Phys. Rev. Lett. **49**, 1947 (1982).
[4] J. Rohler, D. Wohlleben, G. Kaindl, and H. Balster, Phys. Rev. Lett. **49**, 65 (1982).
[5] M. Croft, J. A. Hodges, E. Kemly, A. Krishnan, V. Murgai, and L. C. Gupta, Phys. Rev. Lett. **48**, 826 (1982).
[6] E. Zirngiebl, S. Blumenroder, G. Guntherodt, A. Jayaraman, B. Batlogg, and M. Croft, Phys. Rev. Lett. **54**, 213 (1985).
[7] G. Wortmann, I. Nowik, B. Perscheid, G. Kaindl, and I. Felner, Phys. Rev. B **43**, 5261 (1991).
[8] H. Wada, A. Nakamura, A. Mitsuda, M. Shiga, T. Tanaka, H. Mitamura, and T. Goto, J. Phys.: Condens. Matter **9**, 7913 (1997).
[9] H. Wada, T. Sakata, A. Nakamura, A. Mitsuda, M. Shiga, Y. Ikeda, and Y. Bando, J. Phys. Soc. Jpn. **68**, 950 (1999).
[10] H. Wada, M. F. Hundley, R. Movshovich, and J. D. Thompson, Phys. Rev. B **59**, 1141 (1999).
[11] T. Kinoshita, H. P. J. Gunasekara, Y. Takata, S. Kimura, M. Okuno, Y. Haruyama, N. Kosugi, K. G. Nath, H. Wada, A. Mitsuda, M. Shiga, T. Okuda, A. Harasawa, H. Ogasawara, and A. Kotani, J. Phys. Soc. Jpn. **71**, 148 (2002).
[12] E. R. Bauminger, D. Froindlich, I. Nowik, S. Ofer, I. Felner, and I. Mayer, Phys. Rev. Lett. **30**, 1053 (1973).
[13] O. L. T. de Menezes, A. Troper, P. Lederer, and A. A. Gomes, Phys. Rev. B **17**, 1997 (1978).
[14] F. D. M. Haldane, Phys. Rev. B **15**, 2477 (1977).
[15] J. W. Allen and Richard M. Martin, Phys. Rev. Lett. **49**, 1106 (1982); M. Lavagna, C. Lacroix, and M. Cyrot, Phys. Lett. **90A**, 210 (1982).
[16] G. R. Stewart, Rev. Mod. Phys. **56**, 755 (1984); N. E. Bickers, D. L. Cox, and J. W. Wilkins, Phys. Rev. Lett. **54**, 230 (1985); A. C. Hewson, *The Kondo Problem to Heavy Fermions* (Cambridge University Press, Cambridge, 1993); D. Malterre, M. Grioni, and Y. Baer, Adv. Phys. **45**, 299 (1996); For a concise perspective, see J. W. Allen, G.-H. Gweon, H. T. Schek, L.-Z. Liu, L. H. Tjeng, J.-H. Park, W. P. Ellis, C. T. Chen, O. Gunnarsson, O. Jepsen, O. K. Anderson, Y. Dalichaouch, and M. B. Maple, J. Appl. Phys. **87**, 6088 (2000).
[17] A. N. Tahvildar-Zadeh, M. Jarrell, and J. K. Freericks, Phys. Rev. Lett. **80**, 5168 (1998); W. Chung and J. K. Freericks, *ibid.* **84**, 2461 (2000).
[18] C. Huscroft, A. K. McMahan, and R. T. Scalettar, Phys. Rev. Lett. **82**, 2342 (1999).
[19] N. S. Vidhyadhiraja, A. N. Tahvilder-Zadeh, M. Jarrell, and H. R. Krishnamurthy, Europhys. Lett. **49**, 459 (2000).
[20] S. Burdin, A. Georges, and D. R. Grempel, Phys. Rev. Lett. **85**, 1048 (2000).
[21] J.K. Freericks and V. Zlatic, Rev. Mod. Phys. **75**, 1333 (2003); V. Zlati and J. K. Freericks, Acta Phys. Pol. B **32**, 3253 (Special Issue) (2001).
[22] A. Delin, L. Fast, B. Johansson, J. M. Wills, and O. Eriksson, Phys. Rev. Lett. **79**, 4637 (1997); W. M. Temmerman, Z. Szotek, A. Svane, P. Strange, H. Winter, A. Delin, B. Johansson, O. Eriksson, L. Fast, and J. M. Wills, *ibid.* **83**, 3900 (1999); P. Strange, A. Svane, W. M. Temmerman, Z. Szotek, and H. Winter, Nature (London) **399**, 756 (1999).
[23] C. Lehner, M. Richter, and H. Eschrig, Phys. Rev. B **58**, 6807 (1998).
[24] A. Chainani, H. Kumigashira, T. Ito, T. Sato, T. Takahashi, T. Yokoya, T. Higuchi, T. Takeuchi, S. Shin, and N. K. Sato, Phys. Rev. B **65**, 155201 (2002).
[25] L. Chandran, H. R. Krishna-murthy, and T. V. Ramakrishnan, J. Phys.: Condens. Matter **4**, 7067 (1992).
[26] I. Felner and I. Nowik, J. Phys. Chem. Solids **39**, 763 (1977).
[27] J. Sakurai, S. Fukuda, A. Mitsuda, H. Wada, and M. Shiga, Physica B **281–282**, 134 (2000).
[28] F. Reinert, R. Claessen, G. Nicolay, D. Ehm, S. Hufner, W. P. Ellis, G.-H. Gweon, J. W. Allen, B. Kindler, and W. Assmus, Phys. Rev. B **58**, 12808 (1998), and references therein.
[29] J. J. Yeh and I. Lindau, At. Data Nucl. Data Tables **32**, 1 (1985).
[30] B. Johansson, Phys. Rev. B **19**, 6615 (1979).
[31] N. Martensson, B. Reihl, W.-D. Schneider, V. Murgai, L. C. Gupta, and R. D. Parks, Phys. Rev. B **25** 1446 (1982).
[32] W. D. Schneider, C. Laubschat, G. Kalkowski, J. Haase, and A. Puschmann, Phys. Rev. B **28**, 2017 (1983).
[33] E.-J. Cho, S-J. Oh, S. Suga, T. Suzuki, and T. Kasuya, J. Electron Spectrosc. Relat. Phenom. **77**, 173 (1996).
[34] F. Gerken, J. Barth, and C. Kunz, Phys. Rev. Lett. **47**, 993 (1981); P.A. Cox, Y. Baer, and C.K. Jorgensen, Chem. Phys. Lett. **22**, 8864 (1973); W. Gudat, S.F. Alvarado, and M. Campagna, Solid State Commun. **28**, 943 (1978); T. Jo and A.

Tanaka, J. Phys. Soc. Jpn. **66**, 485 (1997).
[35] H. Yamagami, J. Phys. Soc. Jpn. **68**, 1975 (1999).
[36] D. Ehm, F. Reinert, G. Nicolay, S. Schmidt, S. Hufner, R. Claessen, V. Eyert, and C. Geibel, Phys. Rev. B **64**, 235104 (2001).
[37] M. R. Norman, H. Ding, M. Randeria, J. C. Campuzano, T. Yokoya, T. Takeuchi, T. Takahashi, T. Mochiku, K. Kadowaki, P. Guptasarma, and D. G. Hinks, Nature (London) **392**, 157 (1998); A. Chainani, T. Yokoya, T. Kiss, and S. Shin, Phys. Rev. Lett. **85**, 1966 (2000).